Journal of Organometallic Chemistry, 287 (1985) 357–367
Elsevier Sequoia S.A., Lausanne – Printed in The Netherlands

ADDITION AND ELIMINATION OF HYDROGEN AND LIGAND SUBSTITUTION ON TRIOSMIUM CLUSTERS. KINETICS AND MECHANISM

LYNN M. BAVARO and JEROME B. KEISTER*

Department of Chemistry, State University of New York at Buffalo, Buffalo, New York 14214 (U.S.A.)

(Received November 27th, 1984)

Summary

The kinetics of the reversible reaction $HOs_3(\mu\text{-}COMe)(CO)_{10} + H_2 \rightleftarrows H_3Os_3(\mu_3\text{-}COMe)(CO)_9 + CO$ has been investigated. The reaction of $HOs_3(\mu\text{-}COMe)(CO)_{10}$ with hydrogen involves dissociation of a CO ligand prior to the rate-determining step, which is proposed to be the oxidative addition of molecular hydrogen. The reaction of $H_3Os_3(\mu_3\text{-}COMe)(CO)_9$ with CO involves rate-limiting hydrogen loss. The equilibrium constant and the competition ratio for hydrogen and CO for the unsaturated intermediate were determined. The mechanism of substitution by $AsPh_3$ on $HOs_3(\mu\text{-}COMe)(CO)_{10}$ also involves a CO dissociative mechanism. Based upon relative rate constants for CO, $AsPh_3$, and hydrogen addition to $HOs_3(COMe)(CO)_9$, CO dissociation and hydrogen addition are proposed to occur at different metal sites.

Oxidative addition and reductive elimination of hydrogen are reactions of fundamental importance in homogeneous or heterogeneous catalysis, and while many studies have examined hydrogen activation by monometallic complexes [1], little is known about this process on metal clusters. We recently described the first study of the kinetics of oxidative addition and reductive elimination of molecular hydrogen for a triruthenium cluster system (eq. 1) [2]. Our results indicated dissociative loss of CO during the forward reaction and dissociative loss of hydrogen during the reverse

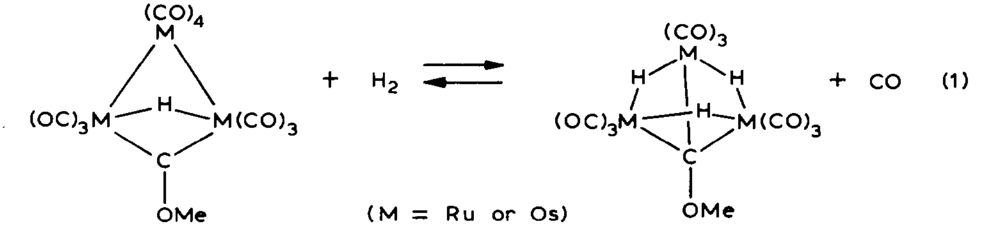

(1)

0022-328X/85/$03.30

process. However, questions regarding the metal site or sites involved in the transition states, the bridging mode of the COMe ligand and the distribution of CO ligands in the intermediate(s) remain unanswered.

One approach to these questions is to examine the kinetics of the analogous processes for heterometallic clusters $HRu_{3-n}Os_n(\mu\text{-}COMe)(CO)_{10}$ and $H_3Ru_{3-n}Os_n(\mu_3\text{-}COMe)(CO)_9$, which should be isostructural with the homometallic analogs but which should display significantly different reactivities for Ru and Os sites. In preparation for such a study we have investigated the hydrogenation of $HOs_3(\mu\text{-}COMe)(CO)_{10}$, the carbonylation of $H_3Os_3(\mu_3\text{-}COMe)(CO)_9$, and ligand substitution on $HOs_3(\mu\text{-}COMe)(CO)_{10}$ by $AsPh_3$. These results, complicated by cluster decomposition, allow semi-quantitative comparisons of the Ru and Os cluster systems and provide a basis for evaluation of data for the mixed cluster systems, the subject of a later paper.

Experimental

Chemicals. Published procedures were used for syntheses of $HOs_3(\mu\text{-}COMe)(CO)_{10}$ [3,4] and $H_3Os_3(\mu\text{-}COMe)(CO)_9$ [3]. An impurity in samples of $HOs_3(\mu\text{-}COMe)(CO)_{10}$ prepared in this manner is $HOs_3(\mu\text{-}OMe)(CO)_{10}$ [5], which is not easily separated from the desired product; however, this impurity did not interfer with the kinetic measurements and so some studies were performed on the mixture. Decane was obtained from Aldrich and used as received. Triphenylarsine was obtained from Alfa and used as received. Hydrogen and CO were supplied by Airco and Linde, respectively. A pre-analyzed mixture of CO (25.0%) and hydrogen (75.0%) was obtained from Linde.

Kinetic measurements. Hydrogenation, carbonylation, and substitution reactions were monitored by infrared spectroscopy (2057 cm^{-1} for $HOs_3(\mu\text{-}COMe)(CO)_{10}$, 2074 cm^{-1} for $H_3Os_3(\mu_3\text{-}COMe)(CO)_9$, and 2109 cm^{-1} for $HOs_3(\mu\text{-}COMe)(CO)_{10}$, respectively) using a Beckman 4240 spectrophotometer kindly supplied by Professor Jim Atwood.

Carbonylation and hydrogenation reactions at greater than 1 atm pressure were conducted in a 300 cm^3 Autoclave Engineers Magnadrive autoclave equipped with a Love Controls Corp. Model 165-766-213 temperature controller ($\pm 1°C$) and a liquid sample system. After bringing the autoclave to the temperature desired, the solution of the starting cluster was injected into the autoclave from a 40 cm^3 bomb. Then liquid samples were periodically removed for analysis. Cluster concentrations were ca. 1.7×10^{-3} *M* in decane.

Reactions at 1 atm were conducted in a flask equipped with gas inlet tube inserted into the solution, reflux condenser, and gas outlet to a bubbler, and immersed in a Haake constant temperature bath ($\pm 0.1°C$). Samples were removed via syringe.

Kinetic studies of substitution on $HOs_3(\mu\text{-}COMe)(CO)_{10}$ were conducted as described for the 1 atm reactions. The initial cluster concentration was 7×10^{-4} *M* in decane. Concentrations of $AsPh_3$ used were 7×10^{-3} to 3.5×10^{-2} *M*.

Rate constants were determined by a computer-calculated least squares fit of plots of ln(abs) vs. time. Two to five measurements were made for each set of conditions. Error limits are given as one standard deviation from the mean.

The equilibrium constant (eq. 2) was determined in the following manner. A solution of $HOs_3(\mu\text{-}COMe)(CO)_{10}$ (56 mg, 0.063 mmol) in decane (100 ml) was placed in the autoclave, which was flushed four times to 70 atm with a CO/hydrogen mixture (25.0/75.0) and then filled to 35 atm. The autoclave was heated to 110°C and maintained at that temperature with stirring for 5 days. At that time monitoring of the reaction by infrared spectroscopy revealed that the relative absorbances of peaks due to $HOs_3(\mu\text{-}COMe)(CO)_{10}$ (2057 cm^{-1}) and $H_3Os_3(\mu_3\text{-}COMe)(CO)_9$ (2074 cm^{-1}) had reached a constant value. The autoclave was rapidly cooled to 25°C. After removal of solvent with vacuum, the residue was dissolved in $CDCl_3$ and analyzed by ^1H NMR spectroscopy; the ratio of the integrals of the hydride resonances gave a molar ratio for $[H_3Os_3(\mu_3\text{-}COMe)(CO)_9]/[HOs_3(\mu\text{-}COMe)(CO)_{10}]$ of 0.25 ± 0.03. Using the CO/H_2 ratio of 0.33, the value for K_{eq} (eq. 2) was calculated as 0.08 ± 0.02.

$HOs_3(\mu\text{-}COMe)(CO)_9(AsPh_3)$. A solution of $HOs_3(\mu\text{-}COMe)(CO)_{10}$, contaminated with $HOs_3(\mu\text{-}OMe)(CO)_{10}$ (total, 51 mg, 0.057 mmol) and $AsPh_3$ (52 mg, 0.18 mmol) in decane was heated at 110°C under nitrogen for 5 h. Then the solvent was removed with vacuum. The residue was purified by thin layer chromatography on silica eluting with 10% dichloromethane in hexane. Products were $Os_3(CO)_{12}$ (band 1, trace), $HOs_3(\mu\text{-}COMe)(CO)_{10}$ (band 2, 7 mg) $Os_3(CO)_{11}(AsPh_3)$ (band 3, 2 mg), $HOs_3(\mu\text{-}COMe)(CO)_9(AsPh_3)$ (band 4, 31 mg, 47%), and $HOs_3(\mu\text{-}OMe)(CO)_9(AsPh_3)$ (band 5, 7 mg, 11%). The remainder could not be identified.

$HOs_3(\mu\text{-}COMe)(CO)_9(AsPh_3)$. IR ($C_6H_{12}$): 2092m, 2050vs, 2014vs, 2008vs, 2001s, 1990m, 1982w, 1972m, 1957w, and 1946m cm^{-1}. ^1H NMR ($CDCl_3$, 25°C): 7.4 (m, 15H), 3.86 (br, 1.6 H), 4.17 (b, 1.4 H), −15.70 (b, 1H) ppm.

$HOs_3(\mu\text{-}OMe)(CO)_9(AsPh_3)$. IR ($C_6H_{12}$): 2096m, 2055s, 2018s, 2011s, 1991w, 1980w, 1974w, and 1948w cm^{-1}. ^1H NMR ($CDCl_3$, 25°C): 7.4 (m, 15 H), 3.14 (s, 3 H), −13.63 (s, 1 H) ppm.

$HOs_3(\mu\text{-}COMe)(CO)_9(PPh_3)$. To a solution of $HOs_3(\mu\text{-}COMe)(CO)_{10}$ and $HOs_3(\mu\text{-}OMe)(CO)_{10}$ (total, 260 mg) in acetonitrile (20 ml) under a nitrogen atmosphere was added trimethylamine-*N*-oxide dihydrate (28 mg) in acetonitrile (50 ml). The solution was stirred for 30 min and then triphenylphosphine (80 mg) in acetonitrile was added. The solution was then evaporated to dryness and the mixture separated by thin layer chromatography on silica eluting with 10% dichloromethane in hexane. The third yellow band was extracted with dichloromethane and then evaporation yielded 102 mg of a mixture of $HOs_3(\mu\text{-}COMe)(CO)_9(PPh_3)$ and $HOs_3(\mu\text{-}OMe)(CO)_9(PPh_3)$ (4/1 ratio). Two further chromatographic separations, taking the upper portion of the band each time, yielded pure $HOs_3(\mu\text{-}COMe)(CO)_9(PPh_3)$ (33 mg). The complex was recrystallized from methanol.

$HOs_3(\mu\text{-}COMe)(CO)_9(PPh_3)$. IR ($C_6H_{12}$): 2090m, 2049s, 2012vs, 2001vs, 1989w, 1982m, 1972w, 1962vw, and 1950vw cm^{-1}. ^1H NMR ($CDCl_3$, −20°C): 7.4 (m, 15 H), 4.16 (s, 1.9 H), 3.63 (s, 1.1 H), −15.62 (d, 0.36 H, *J*(PH) 6.7 Hz), −15.72 (d, 0.62 H, *J*(PH) 6.7 Hz) ppm; ($CDCl_3$, 25°C): 4.17 (s, 2.1 H), 3.69 (br s, 0.9 H), −15.61 (d, 0.3 H, *J*(PH) 7 Hz), −15.68 (d, 0.7 H, *J*(PH) 7 Hz) ppm. EI MS: *m/z* 1134 ($^{192}Os_3$). Anal. Found: C, 30.78; H, 1.74. $C_{29}H_{19}O_{10}Os_3P$ calcd.: C, 30.85; H, 1.70%.

Variable temperature ^1H NMR spectra. The ^1H NMR spectra of $HOs_3(\mu\text{-}COMe)(CO)_9(PPh_3)$ in $CDCl_3$ were examined as a function of temperature using a JEOL FX-90Q spectrometer. Temperature measurements between −20 and 45°C were made using the methanol chemical shift method [6]. Broadening of the methyl resonances for the two isomers near the slow exchange limit [7] was used to estimate the rate constant for exchange from minor to major isomer at 25°C (7 s^{-1}), 35°C (32 s^{-1}), and 44°C (54 s^{-1}) and the rate constant for exchange from major to minor isomer at 35°C (11 s^{-1}) and 44°C (29 s^{-1}). After correction for the free energy difference between the two isomers (0.4 kcal at 25°C) the average of the free energies of activation for minor isomer to major isomer conversion (16.1 ± 0.2 kcal/mol, error limits are one standard deviation) was taken as the best estimate (assuming $\Delta S^{\neq}$ is small so that the values at 25–44°C are within experimental error) of $\Delta G^{\neq}$ (minor → major). The systematic error associated with measurement of the linewidth in the absence of exchange has not been considered.

Results

Ligand substitution on $HOs_3(\mu\text{-}COMe)(CO)_{10}$. In decane solution at 80–110°C $HOs_3(\mu\text{-COMe})(CO)_{10}$ reacts with excess $AsPh_3$ to yield initially $HOs_3(\mu\text{-COMe})(CO)_9(AsPh_3)$, which undergoes further reaction to uncharacterized products, which by analogy to substitutions of $HRu_3(\mu\text{-COMe})(CO)_{10}$ [8] are most likely poly-substituted. The monosubstituted product can be separated by thin layer chromatography from the unreacted material and other products or can be prepared using trimethylamine-*N*-oxide to induce substitution, as was done to prepare $HOs_3(\mu\text{-COMe})(CO)_9(PPh_3)$. Isolated yields of the monosubstituted cluster by either route are not high because of polysubstitution during the thermal reaction and because of side reactions involving attack on the COMe ligand during the trimethylamine-*N*-oxide reaction.

The clusters $HOs_3(\mu\text{-COMe})(CO)_9L$ ($L = AsPh_3$ or PPh_3) have been characterized by infrared and ^1H NMR spectroscopy, mass spectrometry, and elemental analysis. The molecular ion is observed in the EI mass spectrum of $HOs_3(\mu\text{-COMe})(CO)_9PPh_3$. The infrared and ^1H NMR spectra of these two complexes and of the Ru analogs [8] are all very similar and, thus, all are presumed isostructural. The ^1H NMR spectrum of each Os cluster indicates the presence of two isomers, each of which having one methyl group and one hydride ligand; for the PPh_3 derivative each isomer displays an identical coupling constant of 6.7 Hz between ^{31}P and the hydride resonance, suggesting similar orientations of the hydride ligand and PPh_3 ligand in the two. The value for the ^{31}P–hydride coupling constant is very similar to that found for the closely related cluster $HOs_3(\mu\text{-NCHCF}_3)(CO)_9(PMe_2Ph)$ (J(P–H) 8.6 Hz), which was shown by X-ray crystallography to be substituted on a bridged Os atom in a site *cis* to the hydride and *trans* to the $Os(CO)_4$ fragment [9]. This is in fact the most common site for phosphine substitution on $M_3(\mu\text{-X})_2(CO)_{10}$ clusters. Thus, the structures of $HOs_3(\mu\text{-COMe})(CO)_9L$ are proposed to be as shown in Fig. 1.

The two isomers of $HOs_3(\mu\text{-COMe})(CO)_9L$ are assigned to the two rotamers differing in relative orientation of the Me group and L (*syn* and *anti*). For the isostructural $HRu_3(\mu\text{-CNMe}_2)(CO)_9L$ clusters one of the two Me resonances is shifted upfield by 0.6 ppm from the other and from the position of the Me resonance of $HRu_3(\mu\text{-CNMe}_2)(CO)_{10}$; this upfield shift is attributed to ring current effects from the phenyl substituents upon the *syn* Me resonance [8]. On the basis of the upfield shift of the Me resonance due to minor isomer of $HOs_3(\mu\text{-COMe})(CO)_9L$, the *syn* isomer is the less stable one, as expected on steric grounds. The relative ratio

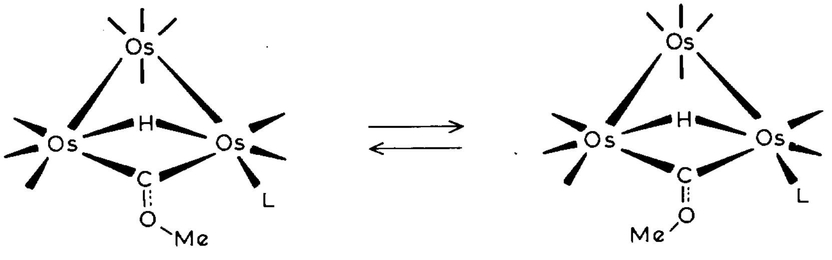

syn anti

Fig. 1. Structures of *syn* and *anti* isomers of $HOs_3(\mu\text{-COMe})(CO)_9L$, L = $AsPh_3$ or PPh_3.

of 2.0 ± 0.2 at 25°C for the Me resonances of the *syn* and *anti* isomers corresponds to a free energy difference of 0.4 kcal between the two rotamers. The ratio of the integrals of the methyl resonances does not vary enough with temperature to allow estimation of ΔH^0 for the isomerization. Exchange broadening of methyl and hydride resonances for each isomer is observed at 25°C; line width measurements at up to 45°C indicate a free energy barrier of 16.1 ± 0.2 kcal/mol at 35°C (average temperature) for *syn* to *anti* isomerization. This may be compared with the free energy barrier of 13.4 kcal/mol for alkyl group flipping in $HOs_3(\mu\text{-COMe})(CO)_{10}$ [4] or $HOs_3(\mu\text{-COEt})(CO)_{10}$ [3,4]. The significantly higher free energy of activation for $HOs_3(\mu\text{-COMe})(CO)_9(PPh_3)$ may be due to steric interactions between the phenyl substituents on phosphorus and the methyl group; the steric crowding must be more significant in the transition state than in the ground state. However, the basis for the variation in activation barrier with ligand properties cannot be evaluated until more examples are investigated.

The kinetics of substitution on $HOs_3(\mu\text{-COMe})(CO)_{10}$ by $AsPh_3$ (10- to 50-fold excess) at 90–110°C was examined. Infrared spectroscopy was used to monitor disappearance of the starting cluster. Plots of ln (absorbance) vs. time were linear for two to three half lives, indicating a rate law first-order in cluster concentration (Table 1). The pseudo-first order rate constants at 90°C were within experimental error independent of the concentration of $AsPh_3$ over the range examined. Under a CO atmosphere the rate was substantially lower, indicating CO inhibition. Activation parameters for disappearance of $HOs_3(\mu\text{-COMe})(CO)_{10}$ were determined to be $\Delta H^{\neq}$ 34.1 ± 0.7 kcal/mol and $\Delta S^{\neq} = +13 \pm 2$ eu. These values may be compared

TABLE 1

RATE CONSTANTS FOR SUBSTITUTION BY $AsPh_3$ ON $HOs_3(\mu\text{-COMe})(CO)_{10}$ [a]

T (°C)	$[AsPh_3]$ (mM)	k_{obs} $(s^{-1}) \times 10^6$
90.0	8.1	19 ± 2
90.0	35	22 ± 3
90.0 [b]	7.0	1.7 [b]
100.0	7.6	66 ± 2
104.1	8.4	120 ± 10
109.9	7.1	230 ± 10

[a] Initial concentration ca. 7×10^{-4} M in decane. [b] Under 1 atm of CO.

with values for the analogous Ru system, $\Delta H^{\neq}$ 26.6 kcal/mol and $\Delta S^{\neq}$ 8 eu [8]. Overall, the data indicate a CO dissociation mechanism for $AsPh_3$ substitution, as was found for the Ru analog, However, CO dissociation from Os is much slower than from Ru, presumably because of the substantially stronger Os–CO bond.

Hydrogenation of $HOs_3(\mu\text{-}COMe)(CO)_{10}$. Unlike conversion of $HRu_3(\mu\text{-}COMe)(CO)_{10}$ to $H_3Ru_3(\mu_3\text{-}COMe)(CO)_9$, hydrogenation of the Os cluster is not a clean reaction. After hydrogenation at 90°C and under 50 atm of hydrogen for 3 days chromatographic separation of one product mixture yielded $H_3Os_3(\mu_3\text{-}COMe)(CO)_9$ (74%), $HOs_3(\mu\text{-}COMe)(CO)_{10}$ (13%), and $H_2Os_3(CO)_{10}$ [10] (11%).

The progress of the hydrogenation was monitored using infrared spectroscopy to measure the concentration of $HOs_3(\mu\text{-}COMe)(CO)_{10}$. As was found for hydrogenation of $HRu_3(\mu-COMe)(CO)_{10}$ [2], linear plots of ln (absorbance) vs. time were not obtained and the curvature of the plots depended upon the experimental set-up. In an open system in which hydrogen (1 atm) was bubbled through the solution, sweeping out released CO, the rate of disappearance of $HOs_3(\mu\text{-}COMe)(CO)_{10}$ increased with increasing conversion, while in the autoclave, a closed system, the rate decreased with increasing conversion (Fig. 2). The maximum slope of the ln (absorbance) plot for the open system at 80–95% conversion was 1×10^{-4} s^{-1} at 90°C, while the maximum slope for the closed system, at the beginning of the reaction, was 1×10^{-5} s^{-1}.

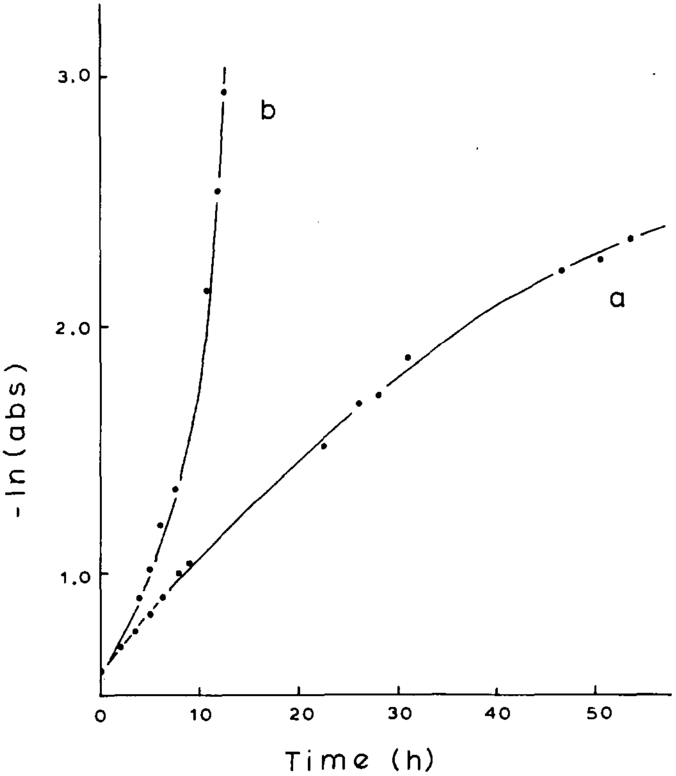

Fig. 2. Plots of $-\ln$ (absorbance) for $HOs_3(\mu\text{-}COMe)(CO)_{10}$ vs. time for hydrogenation at 90°C (a) in the autoclave at 50 atm and (b) with hydrogen bubbled through the solution.

These observations may be explained, as was the case for the Ru system, as being due to inhibition of the hydrogenation by CO produced in the reaction. In the closed system, build-up of CO concentration reduces the rate as the reaction proceeds. With hydrogen bubbling through the solution, no CO build-up occurs, but since CO is not instantaneously removed, the differential concentration of CO is highest when the concentration of $HOs_3(\mu\text{-COMe})(CO)_{10}$ (more properly $HOs_3(COMe)(CO)_9$) is highest, at the beginning of the reaction; the rate thus increases as the amount of $HOs_3(\mu\text{-COMe})(CO)_{10}$ decreases. These observations suggest that the initial step is CO dissociation.

Carbonylation of $H_3Os_3(\mu_3\text{-COMe})(CO)_9$. In decane solution and under 14 to 70 atm of CO, $H_3Os_3(\mu_3\text{-COMe})(CO)_9$ is converted to $HOs_3(\mu\text{-COMe})(CO)_{10}$. However, unlike the analogous reaction for $H_3Ru_3(\mu_3\text{-COMe})(CO)_9$, the carbonylation is accompanied by substantial decomposition to $Os(CO)_5$. In one experiment, (100°C, 91 h, 14 atm) thin layer chromatography of the product mixture yielded $HOs_3(\mu\text{-COMe})(CO)_{10}$ (45%) $H_3Os_3(\mu_3\text{-COMe})(CO)_9$ (34%) and $Os_3(CO)_{12}$ (18%).

The presence of $Os(CO)_5$, (2037, 2000 cm^{-1}) [11] was noted during the carbonylation reaction. At 100°C smooth increases in the absorbances of bands due to $Os(CO)_5$ paralleled the increase in absorbance of $HOs_3(\mu\text{-COMe})(CO)_{10}$. The primary pathway for formation of $Os(CO)_5$ is believed to be reductive elimination of dimethyl ether from $H_3Os_3(\mu_3\text{-COMe})(CO)_9$, rather than fragmentation of $HOs_3(\mu\text{-COMe})(CO)_{10}$. Although the concentration of $HOs_3(\mu\text{-COMe})(CO)_{10}$ does begin to decrease due to fragmentation to presumably $Os(CO)_5$, the approximate rate constant for this process is only 8×10^{-8} s^{-1} (100°C, 70 atm), compared with 2.2×10^{-6} s^{-1} for disappearance of $H_3Os_3(\mu_3\text{-COMe})(CO)_9$. The rate of fragmentation of $H_3Os_3(\mu_3\text{-COMe})(CO)_9$ appears to be faster than the rate of fragmentation of $HOs_3(\mu\text{-COMe})(CO)_{10}$ since the rate of formation of $Os(CO)_5$ begins to decrease as the amount of $H_3Os_3(\mu_3\text{-COMe})(CO)_9$ decreases. Dimethyl ether elimination from $H_3Ru_3(\mu_3\text{-COMe})(CO)_9$ occurs under CO/hydrogen mixtures at temperatures above 100°C, although in the absence of hydrogen the preferred path is hydrogen elimination [3].

Semi-quantitative rate data for the carbonylation was obtained by following the disappearance of the 2074 cm^{-1} band for $H_3Os_3(\mu_3\text{-COMe})(CO)_9$. Plots of ln (absorbance) vs. time were linear for 2.5–3 half lives, indicating that the reaction(s) causing the loss of $H_3Os_3(\mu\text{-COMe})(CO)_9$ is (are) first-order in cluster concentration. Since we cannot accurately correct for the contributions from side reactions, the first order rate constants (Table 2) must be viewed as upper limits for the reaction which forms $HOs_3(\mu\text{-COMe})(CO)_{10}$.

The rate constant for disappearance of $H_3Os_3(\mu_3\text{-COMe})(CO)_9$ is independent of CO pressure between 14 and 70 atm (Table 2). Both hydrogen elimination from $H_3Ru_3(\mu_3\text{-COMe})(CO)_9$ [2] and CH_3X elimination from $H_3Ru_3(\mu_3\text{-CX})(CO)_9$ ($X = CO_2Me$, Ph, or Cl) [12] have been shown to have rate laws which are zero-order in CO pressure. Conversion of $H_3Os_3(\mu_3\text{-COMe})(CO)_9$ by competing pathways to $HOs_3(\mu\text{-COMe})(CO)_{10}$ and to $Os(CO)_5$ and dimethyl ether would be expected to have a rate law zero-order in CO pressure and first-order in cluster concentration, with the first order rate constant representing the sum of the first order rate constants for hydrogen elimination and for dimethyl ether elimination. Based upon the relative amounts of $HOs_3(\mu\text{-COMe})(CO)_{10}$ and $Os_3(CO)_{12}$ formed at 100°C the rate constant for hydrogen elimination must be greater than that for dimethyl ether

TABLE 2

RATE CONSTANTS FOR DISAPPEARANCE OF $H_3Os_3(\mu_3\text{-COMe})(CO)_9$ [a] UNDER CO

T (°C)	P(CO) (atm)	k_{obs} $(s^{-1}) \times 10^6$
100	14	2.1 ± 0.2
100	70	2.2 ± 0.2
110	25	10 ± 1
119	68	26 ± 2

[a] Concentration in decane ca. 7×10^{-4} M.

elimination by a factor of > 2.5. Estimates of the activation parameters for disappearance of $H_3Os_3(\mu_3\text{-COMe})(CO)_9$ (hydrogen elimination and dimethyl ether elimination) are $\Delta H^{\neq}$ 38 kcal/mol and $\Delta S^{\neq}$ 16 eu.

Under a CO-hydrogen mixture an equilibrium between $HOs_3(\mu\text{-COMe})(CO)_{10}$ and $H_3Os_3(\mu_3\text{-COMe})(CO)_9$ was established. Unfortunately, decomposition prevented accurate measurement of the value for the equilibrium constant. However, the steady state ratio of $[H_3Os_3(\mu_3\text{-COMe})(CO)_9]$ to $[HOs_3(\mu\text{-COMe})(CO)_{10}]$, obtained via ^1H NMR spectroscopy of the product mixture after quenching the reaction when no further change was observed in the relative ratio of the infrared absorptions due to the two clusters, suggested an approximate value for K_{eq} (eq. 2) of 0.08 at 110°C, compared with the value of 1.1 at 60°C for the Ru system [2].

$$K_{eq} = \frac{[H_3Os_3(\mu_3\text{-COMe})(CO)_9]\, P(CO)(\text{atm})}{[HOs_3(\mu\text{-COMe})(CO)_{10}]\, P(H_2)(\text{atm})} = 0.08 \pm 0.02 \qquad (2)$$

Discussion

The mechanism previously proposed for the $HRu_3(\mu\text{-COMe})(CO)_{10}/H_3Ru_3(\mu_3\text{-COMe})(CO)_9$ system [2] and described by eq. 3–5 adequately accounts for the substitution kinetics, hydrogenation behavior, and carbonylation kinetics for the analogous Os system. All three reactions are proposed to proceed through an unsaturated intermediate of the composition $HOs_3(COMe)(CO)_9$; however, there may exist isomeric intermediates which may have differing reactivities toward the three substrates.

$$HM_3(\mu\text{-COMe})(CO)_{10} \underset{k_2}{\overset{k_1}{\rightleftharpoons}} HM_3(COMe)(CO)_9 + CO \qquad (3)$$

$$HM_3(COMe)(CO)_9 + H_2 \underset{k_4}{\overset{k_3}{\rightleftharpoons}} H_3M_3(\mu_3\text{-COMe})(CO)_9 \qquad (4)$$

$$HM_3(COMe)(CO)_9 + AsPh_3 \xrightarrow{k_5} HM_3(\mu\text{-COMe})(CO)_9(AsPh_3) \qquad (5)$$

The kinetics of substitution on $HOs_3(\mu\text{-COMe})(CO)_{10}$ by $AsPh_3$ are entirely consistent with a CO dissociative process, as was found for the Ru analog [8]. Thus, the rate law (eq. 6) is zero-order in $[AsPh_3]$ when $[AsPh_3] \gg [CO]$ $(k_5[AsPh_3] \gg k_2[CO])$ and the rate is inhibited when the reaction is conducted under a CO atmosphere $(k_5[AsPh_3] \cong k_2[CO])$. Activation parameters for both Os and Ru systems are similar but the higher $\Delta H^{\neq}$ for the Os cluster is responsible for its substantially slower rate of substitution (at 90°C $k_1(\mathrm{Ru}) = 5 \times 10^{-2}$ s^{-1}, extrapolated from 45°C, vs. $k_1(\mathrm{Os}) = 2 \times 10^{-5}$ s^{-1}).

$$\text{rate of substitution} = \left[\frac{k_1 k_5[\mathrm{AsPh_3}]}{k_2[\mathrm{CO}] + k_5[\mathrm{AsPh_3}]}\right][\mathrm{HOs_3}(\mu\text{-COMe})(\mathrm{CO})_{10}] \tag{6}$$

$$\text{rate of hydrogenation} = \left[\frac{k_1 k_3[\mathrm{H_2}]}{k_2[\mathrm{CO}] + k_3[\mathrm{H_2}]}\right][\mathrm{HOs_3}(\mu\text{-COMe})(\mathrm{CO})_{10}] \tag{7}$$

The initial step for hydrogenation of $\mathrm{HOs_3}(\mu\text{-COMe})(\mathrm{CO})_{10}$ is also proposed to be CO dissociation. Then the limiting rate constant for hydrogenation (at 90°C 1×10^{-5} s^{-1} in the closed system, 1×10^{-4} s^{-1} for the open system) should be the same as the rate constant for $\mathrm{AsPh_3}$ substitution (2×10^{-5} s^{-1} at 90°C) when $[\mathrm{AsPh_3}]$ is large compared to [CO]. These values compare reasonably well, since the initial slope of the ln(abs) plot for the hydrogenation in the closed system is undoubtedly reduced from the true limiting value by CO inhibition and the error associated with the measurements of the slope from hydrogenation in the open system near the end of the reaction is quite large.

Although the unsaturated intermediate $\mathrm{HOs_3(COMe)(CO)_9}$ reacts rapidly with $\mathrm{AsPh_3}$ under pseudo first-order conditions (eq. 6, $k_5[\mathrm{AsPh_3}] \gg k_2[\mathrm{CO}]$), the rate of hydrogen addition to this intermediate is not fast enough to compete with recombination of the intermediate with CO even under 60 atm of hydrogen (eq. 7, $k_3[\mathrm{H_2}] \cong k_2[\mathrm{CO}]$). There is no requirement that hydrogen addition, CO recombination, or $\mathrm{AsPh_3}$ addition all occur at the same metal site. Two or more isomeric intermediates may exist which differ in the arrangement of ligands and in their reactivities toward these substrates. The site of CO dissociation cannot be determined from the position of $\mathrm{AsPh_3}$ substitution since the unsaturated intermediate may be fluxional on the timescale of the reaction and microscopic reversibility does not require $\mathrm{AsPh_3}$ to occupy the site vacated by CO. In fact, the CO ligands of $\mathrm{HOs_3}(\mu\text{-COMe})(\mathrm{CO})_{10}$ are fluxional on the NMR timescale at 60°C [4].

The initial step in carbonylation of $\mathrm{H_3Os_3}(\mu_3\text{-COMe})(\mathrm{CO})_9$ to $\mathrm{HOs_3}(\mu\text{-COMe})(\mathrm{CO})_{10}$ is presumably reductive elimination of hydrogen, as was found for the Ru analog [2]. The rate constant for disappearance of $\mathrm{H_3Os_3}(\mu_3\text{-COMe})(\mathrm{CO})_9$ is independent of the CO pressure, as was found for the Ru analog. Although the activation parameters for disappearance of $\mathrm{H_3Os_3}(\mu_3\text{-COMe})(\mathrm{CO})_9$ cannot be attributed to elimination of hydrogen alone, the values are consistent with rate-determining hydrogen elimination. However, the rate for the Os system is much slower than for the Ru analog (at 100°C $k_4(\mathrm{Ru}) = 4 \times 10^{-4}$ s^{-1} (extrapolated from 80°C) vs. $k_4(\mathrm{Os}) < 2 \times 10^{-6}$ s^{-1}).

As was found for the Ru system, the rate of CO dissociation from $\mathrm{HOs_3}(\mu\text{-COMe})(\mathrm{CO})_{10}$ is much faster than that of hydrogen elimination from $\mathrm{H_3Os_3}(\mu_3\text{-COMe})(\mathrm{CO})_9$. Thus, $k_1/k_4 > 23$ for the Os system at 110°C, compared with $k_1/k_4 \sim 1800$ for the Ru system at 40°C; since for both systems $\Delta H^{\neq}$ is larger for hydrogen elimination than for CO dissociation, this ratio should decrease with increasing temperature. Using the estimated value for K_{eq} (eq. 2) as 0.08 and the calculated ratio of the Henry's Law constants for CO and $\mathrm{H_2}$, $K(\mathrm{CO})/K(\mathrm{H_2})$, of 2.3 at 110°C in decane [13], the competition ratio k_3/k_2 can be estimated as $< 8 \times 10^{-3}$, quite similar to the value for the Ru system at 60°C, 1.4×10^{-3}. Thus, a very unfavorable competition ratio for hydrogen to CO is a characteristic of this reaction for both the Ru and Os clusters.

Competition ratios for monometallic and for polymetallic unsaturated intermediates are usually close to 1, the unsaturated intermediates being relatively non-selective. For example, the competition ratio corresponding to k_3/k_2 for hydrogen and $P(OMe)_3$ for $[Co(P(OMe)_3)_4]^{1+}$ is 1.7 [15]. Competition ratios determined for addition of Lewis bases to unsaturated metal centers are also close to 1. Values of 0.65 for $k(CO)/k(AsPh_3)$ for addition of these ligands to $Mo(CO)_4(PPh_3)$ [16] and of 3 for $k(CO)/k(PPh_3)$ for addition to $Ru_3(CO)_{11}$ [17] are representative.

Although $HM_3(COMe)(CO)_9$ shows an unusually high selectivity for CO addition over hydrogen addition, there is nothing unusual about its selectivity toward other Lewis bases. An estimate of the competition ratio of CO to $AsPh_3$, k_2/k_5, may be obtained from the initial rate constant at 90°C for $AsPh_3$ substitution under an atmosphere of CO. Using the measured value of 1.7×10^{-6} s^{-1}, $k_1 = 2 \times 10^{-5}$ s^{-1}, $[AsPh_3] = 7 \times 10^{-3}$ M, the estimated $[CO] = 1 \times 10^{-2}$ M, and eq. 6, the value obtained for k_2/k_5 is ca. 8. More accurate measurements for the analogous Ru system found a value for $k(CO)/k(PPh_3)$ of 1 [8]. Thus, both $HOs_3(COMe)(CO)_9$ and $HRu_3(COMe)(CO)_9$ are relatively unselective toward the addition of Lewis bases. The source of the small values for k_3/k_2 must arise in hydrogen addition alone.

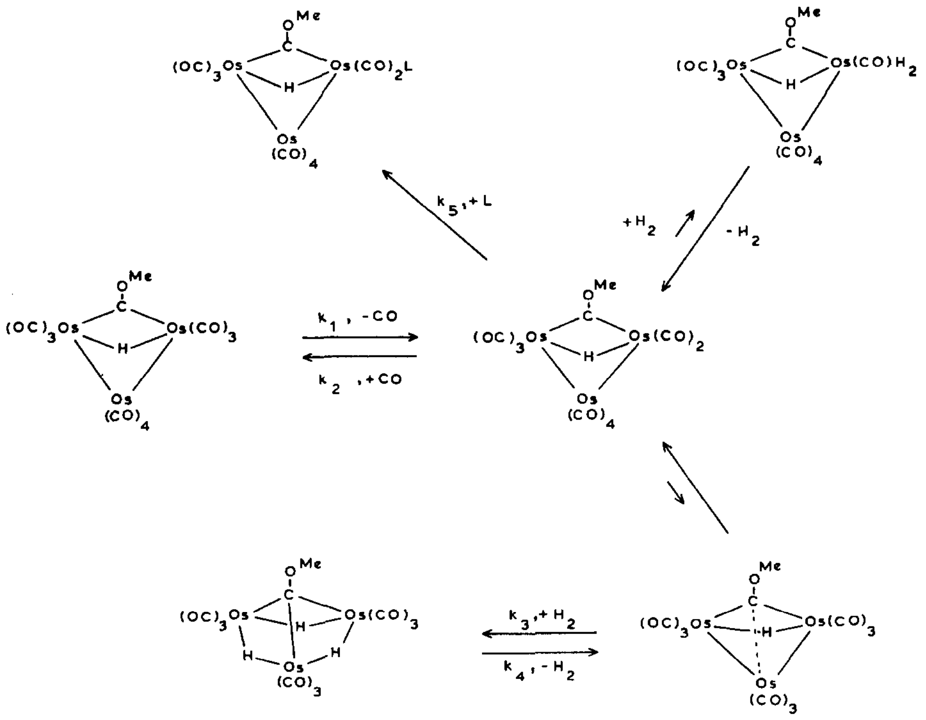

Fig. 3. Proposed mechanisms for hydrogenation and ligand substitution reactions of $HOs_3(\mu\text{-}COMe)(CO)_{10}$ to $H_3Os_3(\mu_3\text{-}COMe)(CO)_9$ and $HOs_3(\mu\text{-}COMe)(CO)_9L$, respectively.

We have suggested that the unusual relative rates for CO addition and hydrogen addition to these unsaturated intermediates may arise from the existence of two isomeric intermediates differing in the location or coordination of the unsaturated metal site (Fig. 3). These two isomeric intermediates might each be rather unselective toward hydrogen or CO addition, but because of very different product stabilities with respect to hydrogen or CO loss only one isomer would form the $H_3M_3(\mu_3$-COMe$)(CO)_9$ product observed. Dramatically different stabilities for MCO or MH_2 complexes are often observed. For example, $Fe(CO)_5$ does not lose CO below 90°C [18] but hydrogen elimination from $H_2Fe(CO)_4$ has a rate constant of 3×10^{-2} s^{-1} at 45°C [19]. The unique aspect of the cluster reaction is that the two metal sites of dramatically different reactivities are in the same molecule.

This unique feature of cluster reactivity may be utilized with heterometallic clusters as catalysts. The coupling of a substitutionally labile metal with an inert metal having significantly different catalytic properties may increase the activity of the catalyst above that found for homometallic clusters. Studies of mixed metal cluster analogs of $HM_3(\mu$-COMe$)(CO)_{10}$ and $H_3M_3(\mu_3$-COMe$)(CO)_9$ are in progress.

Acknowledgement

We owe a great debt to Professor Jim Atwood for helpful discussions and for allowing us to use his infrared spectrophotometer. This work was funded by the National Science Foundation through grant no. CHE 8121059.

References

1 (a) J.O. Noell and P.J. Hay, J. Am. Chem. Soc., 104 (1982) 4578; (b) J.-Y. Saillard and R. Hoffmann, ibid., 106 (1984) 2006 and references therein.
2 L.M. Bavaro, P. Montangero and J.B. Keister, J. Am. Chem. Soc., 105 (1983) 4977.
3 (a) J.B. Keister, M.W. Payne and M.J. Muscatella, Organometallics, 2 (1983) 219; (b) J.B. Keister, J. Chem. Soc., Chem. Comm., (1979) 214.
4 P.D. Gavens and M.J. Mays, J. Organomet. Chem., 162 (1978) 389.
5 B.F.G. Johnson, J. Lewis and P.A. Kilty, J. Chem. Soc. A, (1968) 2859.
6 (a) A.L. Van Geet, 40 (1968) 2227; (b) 42 (1970) 679.
7 T.J. Swift, in G.G. Hammes (Ed.), Investigation of Rates and Mechanisms of Reactions, Techniques of Chemistry, Vol. 6, pt. 2, Wiley Interscience, 1974, p. 521–563.
8 D.M. Dalton, D.J. Barnett, T.P. Duggan, J.B. Keister, P.T. Malik, S.P. Modi, and S.A. Smesko, Organometallics, in press.
9 (a) R.D. Adams, D.A. Katahira and L.-W. Yang, J. Organomet. Chem., 219 (1981) 85; (b) 219 (1981) 241; (c) R.D. Adams and N.M. Golembeski, J. Am. Chem. Soc., 101 (1979) 2579.
10 S.A.R. Knox, J.W. Koepke, M.A. Andrews and H.D. Kaesz, J. Am. Chem. Soc., 97 (1975) 3942.
11 F. Calderazzo and F. L'Eplattenier, Inorg. Chem., 6 (1967) 1220.
12 T.P. Duggan, D.J. Barnett, M.J. Muscatella and J.B. Keister, unpublished results.
13 A formula for the solubilities of CO and hydrogen in non-polar solvents has been provided by Gjaldbaek [14]. For estimations of solubilities in decane we used values for solvent parameters of $\delta_1 = 8$ and $V_1 = 195$.
14 J.C. Gjaldbaek, Acta Chem. Scand., 6 (1952) 623.
15 E.L. Muetterties and P.L. Watson, J. Am. Chem. Soc., 100 (1978) 6978.
16 C.L. Hyde and D.J. Darensbourg, Inorg. Chem., 12 (1973) 1286.
17 A. Poë and M.V. Twigg, J. Chem. Soc., Dalton Trans., (1974) 1860.
18 E.E. Siefert and R.J. Angelici, J. Organomet. Chem., 8 (1967) 374.
19 R.G. Pearson and H. Mauerman, J. Am. Chem. Soc., 104 (1982) 500.